



HAL
open science

Formation of the Moho transition zone in the Oman ophiolite, and comparison with sub-Moho melt lenses at fast spreading ridges

David Jousselin, Adolphe Nicolas, Françoise Boudier, Laurie Reisberg, Mathilde Henri, Marie Nicolle

► To cite this version:

David Jousselin, Adolphe Nicolas, Françoise Boudier, Laurie Reisberg, Mathilde Henri, et al.. Formation of the Moho transition zone in the Oman ophiolite, and comparison with sub-Moho melt lenses at fast spreading ridges. *Tectonophysics*, 2021, 821, pp.229148. 10.1016/j.tecto.2021.229148 . insu-03712881

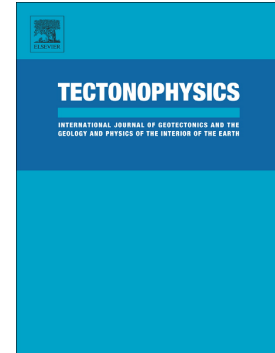
HAL Id: insu-03712881

<https://insu.hal.science/insu-03712881>

Submitted on 22 Nov 2022

HAL is a multi-disciplinary open access archive for the deposit and dissemination of scientific research documents, whether they are published or not. The documents may come from teaching and research institutions in France or abroad, or from public or private research centers.

L'archive ouverte pluridisciplinaire **HAL**, est destinée au dépôt et à la diffusion de documents scientifiques de niveau recherche, publiés ou non, émanant des établissements d'enseignement et de recherche français ou étrangers, des laboratoires publics ou privés.



Formation of the Moho transition zone in the Oman ophiolite, and comparison with sub-Moho melt lenses at fast spreading ridges

David Jousselin, Adolphe Nicolas, Françoise Boudier, Laurie Reisberg, Mathilde Henri, Marie Nicolle

PII: S0040-1951(21)00430-3

DOI: <https://doi.org/10.1016/j.tecto.2021.229148>

Reference: TECTO 229148

To appear in: *Tectonophysics*

Please cite this article as: D. Jousselin, A. Nicolas, F. Boudier, et al., Formation of the Moho transition zone in the Oman ophiolite, and comparison with sub-Moho melt lenses at fast spreading ridges, *Tectonophysics* (2021), <https://doi.org/10.1016/j.tecto.2021.229148>

This is a PDF file of an article that has undergone enhancements after acceptance, such as the addition of a cover page and metadata, and formatting for readability, but it is not yet the definitive version of record. This version will undergo additional copyediting, typesetting and review before it is published in its final form, but we are providing this version to give early visibility of the article. Please note that, during the production process, errors may be discovered which could affect the content, and all legal disclaimers that apply to the journal pertain.

Formation of the Moho transition zone in the Oman ophiolite, and comparison with sub-Moho melt lenses at fast spreading ridges

David Jousset^{1*}, Adolphe Nicolas², Françoise Boudier², Laurie Reisberg¹, Mathilde Henri¹, and Marie Nicolle¹

¹ *Université de Lorraine, CRPG, 54501, Vandoeuvre les Nancy, France*

² *Géosciences, Université de Montpellier 2, CNRS, 34095 Montpellier, France*

* *Corresponding author*

ABSTRACT

Our knowledge of melt distribution in the lower crust and upper mantle at oceanic fast spreading centers is very limited. Evidence of melt accumulation, sometimes away from the axis, has been imaged and interpreted at the Moho of the East Pacific Rise; but the detailed structures of these deep magma lenses remain much more difficult to unveil than that of the shallow axial melt lens at the top of the plutonic crust. Ophiolites offer on-land sections of oceanic lithosphere that can complement marine geological and geophysical observations. We present results of a geological survey of the Moho transition zone at a paleosspreading center in the Oman ophiolite. We find that the thickness of this dunite-rich horizontal layer increases from a few meters at the axis to hundreds of meters 6 km away from the axis, and is reduced to a few meters 2-3 km further away. The base of the Moho transition zone contains dunite and very depleted harzburgite with isotropic plagioclase and clinopyroxene impregnations, and stockwork-like magmatic breccia, indicative of episodic high melt fractions. We conclude that the melt-free dunite horizontal layer may stop the progression of ascending melt; this lead to melt accumulation within the uppermost harzburgite beneath the Moho transition zone and forms the isotropic impregnations. As the melt

dissolves the harzburgite orthopyroxene, and is flushed to the top of the MTZ through the breccia, it leaves new dunite at the base of the Moho transition zone. Repetition of this process renders the Moho transition zone thicker as it moves away from the ridge axis, until it leaves the main area of mantle melt delivery. Then, tectonic thinning and intrusion of parts of the MTZ into the lower crust reduce the MTZ thickness. These processes seem coherent with several marine geophysical observations.

Keywords: Moho, dunite, melt, mantle, oceanic ridges, ophiolites

1. INTRODUCTION

Magma erupted during volcanic events at fast spreading ridges are thought to derive from a melt lens, 0.5-4 km wide and several tens of meters thick, located at the base of the sheeted dike complex, centered beneath the ridge (Kent et al, 1993). Recent studies detail variations in space and time of the size and melt fraction of this shallow axial melt lens (Xu et al, 2014; Marjanovic et al, 2015), and show that ridge segmentation is related to these variations. However, as this melt rises from below, melt distribution near the Moho may be the real controlling factor of the tectonic and magmatic segmentation (Carbotte et al, 2013). Seismic imaging (Barth et al, 1991), compliance studies (Clawford and Webb, 2002), and tomographic imaging (Toomey et al, 2007) point to melt accumulation in the upper mantle, which appears to be segmented, and not always centered beneath the ridge. Despite recent progress in multichannel seismic techniques (Aghai et al, 2014), it remains difficult to image the Moho structure and melt distribution at this depth, in as much detail as the upper-crust axial melt lens. A complementary view of the oceanic lithosphere is provided by ophiolites, even though questions remain about the exact geodynamic settings in which ophiolites are created.

Because of its continuous crustal section with limited faulting, the Oman ophiolite is

considered as an obducted piece of a fast spreading center, with a permanent magma chamber. A dating study shows half-spreading rates of 5-10 cm/yr (Rioux et al, 2012). Above the sheeted dike complex, the basaltic unit (V1, Geotimes Unit), displays MORB-like compositions (Ernewein et al, 1988; Godard et al, 2006). This unit is overlain by hydrothermal deposits and a later basaltic unit (V2, Lasail unit) with island-arc affinities (Alabaster et al, 1982; Ernewein et al, 1988). This prompted the idea that the ophiolite formed in a supra subduction setting. These upper lavas are associated to gabbro-norite, clinopyroxene-rich cumulate, and andesitic dikes that intrude the V1-related layered gabbros (Adachi and Miyashita, 2003). As the V2-related magmatism clearly postdates most of the crustal accretion, and is mostly found in Northern Oman, the geodynamic context of the ophiolite-crustal accretion has long been discussed. Reexamination of the major element compositions of the V1-Geotimes unit shows fractionation trends in a hydrous system, similar to backarc basin and forearc volcanics (MacLeod et al, 2013); new mapping reveals the presence of Lasail-like lava flows intercalated within the Geotimes unit (Belgrano and Diamond, 2019); and a dating study shows that the metamorphic sole predates magmatic rocks (Guilmette et al, 2018). This strongly suggests that the entire ophiolite formed at a paleospreading center, which was active above a subducted slab. The importance of this concern is probably limited when investigating ridge accretion processes because structure, kinematics, buoyancy contrast, and thermal conditions, are similar in backarc and oceanic spreading. The most critical parameters that shape ridge structures are the spreading rate and the presence or absence of a magma chamber (Small, 1994). This is the case even in well-developed backarc basins, where axial depth and segmentation patterns are similar to that occurring on mid-ocean ridges (Taylor et al, 1996). Even though the addition of water should influence viscosity, solidus, and mineral saturation temperatures, it does not seem to fundamentally change the ridge dynamic; what it does is enhance the melt production in the melting region, potentially shaping a slow spreading center with an axial high, instead of an axial valley (Taylor and Martinez, 2003). We thus infer that

observations in the Oman ophiolite that are associated to the V1-Geotimes magmatism, and the asthenospheric mantle flow, are applicable to other cases of fast spreading centers with sustained melt production. Indeed, a wealth of studies in the Oman ophiolite has provided advances in the understanding of fast spreading ridge-related processes; many have been a source of mutually beneficial and constructive debates with the marine geological and geophysical communities. For example, the coherency of several findings at the fast spreading East Pacific rise and the Oman ophiolite is reviewed and discussed by Nicolas and Boudier (2015a).

Relics of melt accumulation beneath the crust have been described in the Oman ophiolite within a horizon referred to as the Moho transition zone (MTZ) (Boudier and Nicolas, 1995). This is a one-meter to a thousand meters thick zone, composed of dunite, with plagioclase and clinopyroxene impregnated dunite, layered gabbro lenses and residual harzburgite. Interfingering relationships between harzburgite and dunite in the lowermost MTZ, and dunite with orthopyroxene relics, suggest a melt-peridotite reactional origin for the dunite (Nicolas and Prinzhofer, 1983). The penetrative structures that mark the asthenospheric mantle flow-field are continuous through harzburgite-dunite boundaries. Petrography and mineral chemistry also show that dunite is a reaction product of harzburgite with a MORB-like orthopyroxene-undersaturated melt (e.g. Kelemen et al, 1995; Akizawa and Arai, 2009). For example, the olivine Mg# $[=Mg/(Mg+Fe_{total})_{at}]$ is very similar in the MTZ dunite and the underlying harzburgite, while olivine in cumulate dunite should have lower Mg#, and residual olivine in dunite formed from very high degree of partial melting should have higher Mg# (Koga et al, 2001). Thus few if any dunitites are residual or cumulate, and most of the dunite is a product of melt/rock reactions with orthopyroxene dissolution of the shallowest harzburgite. As in other ophiolites (Nicolas and Violette, 1982; Nadimi, 2002), thick (>50 meters) MTZs are associated to 5-10 km wide mantle diapirs. The best example of a thick MTZ in the Oman ophiolite is in the Maqsad diapir region (Jousselin et al, 1998), where the crust-mantle interface (Moho) is nearly horizontal, and the

sheeted dikes are vertical, thus preserving original orientations.

In order to understand how the MTZ is accreted, and what is the Moho structure at a fast spreading center, we present a lithological and structural survey of the crust-mantle boundary and the underlying Moho transition zone (MTZ) in the Maqsad area, which is interpreted as a paleospreading center. Old and new structural data are presented to confirm the presence of a mantle diapir, and precisely determine the location of the paleoridge. A map of the thickness of the MTZ in this diapiric area, is presented with 15 detailed logs of the MTZ. Together, these data suggest a model where successive pulses of magmatic underplating, and interaction with the host harzburgite, thicken the MTZ as it drifts away from the ridge axis. When the MTZ is too far from the axis to collect further melt, tectonic thinning, and injection of MTZ material in the crust reduce its thickness. We compare our data with marine geophysical observations and find that our model seems coherent with several processes unveiled at the East-Pacific Rise.

2. GEOLOGICAL SETTING AND RIDGE AXIS LOCATION

The Oman ophiolite was emplaced as a >10 km thick nappe. Low temperature deformation associated with its detachment or later deformation overprinting primary features, is readily identified because it is associated to fine grained porphyroclastic textures with strong degrees of recrystallization into neoblasts. Global mapping show that this type of deformation is mostly restricted to the base of the ophiolite (Fig. 1a). Also, even though many fractures can be found at the sample scale, high temperature penetrative flow fields and the Moho show very little displacement at scales from tens of meters to an entire massif, except for a few well identified faults. Inside the massifs, asthenospheric and magmatic structures that formed at, and drifted away from, a paleospreading center are therefore preserved, unmodified through obduction (Nicolas and Boudier, 1995). Independent of the geodynamic context of the spreading center, the short time span between igneous crystallization of the ophiolite and the formation of its metamorphic sole

constrains the location of intra oceanic thrusting to the region adjacent to the paleospreading center (Boudier et al, 1988; Hacker, 1994, Warren et al, 2005). The discovery of several mantle diapirs, aligned parallel to the NW-SE sheeted dike system along the southern part of the ophiolite belt, suggested the possibility that the ridge itself was sampled within the ophiolite (Nicolas et al, 1988). The diapirs were defined by irregular clusters of steeply plunging lineations, rimmed by horizontal lineations, with varying azimuths suggesting a radial flow outward from the diapir, correlated with evidences of local intense magmatic activity, such as numerous dikes and a >100 meters thick MTZ beneath the crust, not seen in other areas (Nicolas et al, 1988; Jouselin et al, 1998). Nicolas and Boudier (1995) provided three independent ways of defining the location of the paleo ridge axis: (1) as a line through a diapir core parallel to the sheeted dike complex; (2) as a limit between opposed shear senses for horizontal lineations in the mantle; (3) as a limit between opposed dipping directions for the foliation of the upper gabbros. These have proved to be strongly coherent for the Nakhl diapir (Nakhl-Rustaq massif) and the Maqsad diapir (Sumail massif), as, within each of the diapirs, the three methods define similar NW-SE lines with variations contained in < 2 km wide bands. Also, this axis seems continuous from one diapir to the other. Another axis was suggested in the Wadi Tayin massif, going through the Batin diapir (Boudier et al, 1997). This inferred location has been confirmed by both a detailed geochronological study through a west-east section showing the youngest age near the proposed axis location (658471 UTM (E)) with increasing ages outward (Rioux et al, 2012), and by a structural study of the upper gabbro section (Nicolas and Boudier, 2015b). Following the definition of the ridge axis at the diapir scale, the ridge segment geometry was defined based on the orientations of the sheeted dike complex and dikes in the mantle in the southern massifs (Boudier et al, 1997). While the center of the ophiolite contains NW-SE dikes, it is bounded on both sides of the Sumail massif by a NE-SW dike system (Fig. 1a). Cross-cutting field relationships seen at the boundaries show that this NE-SW system is older than the central NW-SE

system. This appears possible only if a center of accretion opened between those two boundaries and produced a 50 km wide portion of new lithosphere, nearly centered on the Maqsad diapir. This complex, yet realistic geometry is interpreted as relics of a microplate (Boudier et al, 1997).

Several other pieces of evidence further suggest that most diapirs, including Maqsad, underlay a ridge axis and were not off-axis. Major and rare earth element peridotite compositions of the on-axis Maqsad and Nakhil diapirs confirm that they are areas of high melt flow (Godard et al, 2000). Since the layered gabbros above these areas show no secant intrusions, the melt extracted from the diapirs had to be emplaced when the layered gabbros were forming, thus presumably at the ridge axis, or close enough that the gabbros were not crystallized. The layered gabbros at the base of the crust are magmatically deformed (i.e. without any crystal internal deformation, and with a shape preferred orientation of crystals, ascribed to flow in a dense suspension), with a lineation parallel to that of the plastic lineation of the uppermost peridotite. This shows that their deformation is contemporaneous (Nicolas, et al, 1994). The diapir plunging lineations rotate to the horizontal with the plunge progressively decreasing outward from the diapir; while this fan-shaped geometry is not well understood, this structural continuity from vertical to horizontal flow illustrates that diapirs, with peridotite flowing under asthenospheric condition, reached the base of the crust (Jousselin et al, 1998). Asthenospheric flow, at such shallow depth beneath the crust, is only possible at the rise, where there is no frozen lithospheric mantle in between the crust and the flowing mantle. On the other hand, an off-axis diapir found in the Mansah region (Jousselin and Nicolas, 2000a) has contrasting characteristics. In this case, the steeply plunging lineations are separated from horizontal lineation by a shear zone, which is interpreted as the result of the impingement of the diapir on the off-axis laminated lithospheric mantle. The crust immediately above the off-axis diapir is broken, with tectonic brecciation, and is heavily affected by hydrothermal alteration. Moreover, around and above the off-axis diapir, but not within the diapir itself, the mantle and the lower crust are intruded by microgabbroic dikes and

bodies, which show that magma extracted from the diapir was emplaced in a frozen and cooled lithosphere. Similar intrusions are not reported elsewhere. A geochemical study also illustrates the contrast between the on-axis Maqsad diapir, which carries a MORB-like ϵNd signature, while rocks of the off-axis Mansah diapir indicate a less depleted mantle source (Nicolle et al, 2016).

In Jousselin et al (1998), we detailed the irregular shape of the on-axis Maqsad diapir, and discussed the location of the axis in this area. Together with the use of previous criteria, we associated the axis to a ≈ 500 m wide band where lineations are parallel to the ridge trend, as it is argued that ridge parallel flow should be restricted to the ridge axis (Fig. 1b). Seventy-five new field stations confirm the predictive value of the 1998 structural map made from 460 lineation measurements. In detail, we moved the ridge axis ≈ 730 meters to the north-east compared to past studies (Jousselin et al, 1998; 2003) to adjust for the new lineation measurements, and new data on the Moho transition zone thickness (see below). However a precision smaller than the kilometer scale is probably elusive, as volcanic activity on the surface spans a one kilometer width, and the axis at depth should probably be defined as a broad zone rather than a precise line.

3. RESULTS

3.1. Moho transition zone thickness variations

Prior to our field survey, we tried to pick the base and summit of the MTZ, which is also the base of the crust (the Moho), from aerial photographs available in Google Earth, with help from the BRGM-Oman ministry of Industry geological map (1986-1987), and a compilation of our previous field investigations (Nicolas and Boudier, 1995; Jousselin et al, 1998; Nicolle et al, 2016). Our field survey includes 15 logs where the altitudes of the base of the MTZ and of the Moho, are well constrained by on-site Global Positioning System measurements. Cross examination of the work on the aerial photograph with the field survey results shows that we were able to consistently pick the Moho, but not the base of the MTZ, which needs to be precisely

located in the field to constrain its altitude. Thus we added to our 15 logs 24 sites where we found the base of the MTZ in the field, and we picked the Moho on aerial photographs, permitting us to constrain the MTZ thickness at 39 locations, with a 1-20 meter precision (Fig. 1b). Also, less precise picking of the MTZ limits on aerial photographs throughout the entire region allowed us to build a three dimensional digital model of the bottom and top surfaces of the MTZ. All the logs (Fig. DR1a), the position of transects (Fig. DR1b), further details on the methods, and illustrations of the MTZ three dimensional digital model (Fig. DR2) are given in the Supplemental Information section.

In Fig. 2, we plot the MTZ thickness against the distance from the ridge. The striking result is that the MTZ thickness is thin (≈ 20 meters) beneath the ridge axis, grows to a maximum (450 meters) 6 kilometers away from the axis, before thinning again with increasing distance from the axis. Eight kilometers away from the ridge, the MTZ is 30 meters thick or less. At the scale of the Maqсад area, this thickness reduction seems supported by only three sites (one outside of the map of Fig.1). That is because, away from the Maqсад diapir plateau, which offers multiple topographic outliers where the Moho can be observed, the interception of the Moho and of the topographic surface forms only a line, which does not offer various points of observation. However, larger scale mapping has repeatedly shown that away from mantle diapirs, the MTZ is consistently thin (< 50 meters) (Nicolas et al, 1996). About 70-80% of the ophiolite belt is associated to a thin MTZ. These areas show horizontal mantle flow structures, with lineation azimuth consistently trending at a high angle with the azimuth of the sheeted dike complex, as is expected for mantle flow on the ridge flanks. Prime examples of thin MTZs are the well studied Wadi Al Abyad ("Bani Kharus" in Juteau et al, 1988a) in the Nakhl massif, with a 5-10 meters thick MTZ (at $23^{\circ}26'N-57^{\circ}40'05"E$ and $23^{\circ}26'37"N-57^{\circ}39'26"E$), and the MTZ of the Hilti massif (Ildefonse et al, 1995).

3.2. Structure and lithologies of the MTZ

The 15 logs of the MTZ are presented in Figure DR1a, with a selection in Fig.3, which shows the main features, and is arranged at increasing distance from the ridge axis from left to right. Fig.4 shows field observations, with an emphasis on new observations (Fig.4 c-f).

3.2.1. Results consistent with previous studies.

The logs contain all the classic lithologies described in Boudier and Nicolas (1995), that is dunite, plagioclase and clinopyroxene bearing dunites called impregnated dunite, layered gabbro lenses in dunite, few chromite pods, ultramafic intrusions in the lower crust that are rooted in the MTZ or transposed in the lower layered gabbros, and centimetric to metric patches of harzburgite within the dunite. Here we mostly describe the frequency of these classic lithologies rather than describe individual logs, as no systematic evolution in occurrences of these facies can be found from one log to the other. All the logs show the prominence of the dunite component (<95% of the MTZ). Except in the case of dunite with isotropic impregnations (see below), all the dunites show an asthenospheric planar and linear structure marked by spinel grains, usually visible on saw-cut samples bleached with diluted hydrochloric acid. Sometimes the spinel grains are very small, which make the structure difficult to see, however the thin sections show porphyroclastic textures, with a strong crystallographic preferred orientation (most grains have a similar angle of extinction under polarized light). A small part of the dunites and impregnated dunites (17 samples out of 128 in thin sections) contains small isolated orthopyroxene grains with corroded boundaries, which represent a transitional stage from harzburgite to dunite, formed by reactive dissolution of orthopyroxene (figure 9 in Boudier and Nicolas, 1995). This can be found near the top of the MTZ (Fig. 4a, Fig. DR3, 50m beneath the Moho within a 450m thick MTZ), or near the base, as in the isotropic impregnations of the Mahram outcrop (Fig. 1 and 3). Beside these observations at the thin section scale, about half of the logs show clear centimetric patches or centimetric to metric

bands of harzburgite within the first 25 meters at the base of the MTZ, and few bands of dunite in the shallowest harzburgite. This forms a gradational contact between the MTZ and the underlying harzburgite. In the other half of the logs, the base of the MTZ is sharp. A third of the logs contain a few outcrops with centimeter to meter scale layered gabbro lenses in the dunite; the maximum thickness of gabbro lenses is of the order of 10 meters (cross-section 11OD10, and near the oasis of Tuff at 23°06'13.7"N, 57°57'19.7"E, figure 2.2 in Boudier and Nicolas, 1995). Half of the logs show dunites impregnated with plagioclase and/or clinopyroxene, dispersed within layers several centimeters or meters thick, which are often too thin to be well represented on logs at the scale of several tens of meters. These impregnations can be found at any height within the MTZ section, with no particular systematics. Plagioclase and clinopyroxene grains display no intracrystalline deformation, but they do have a shape fabric, parallel to the spinel-marked plastic lineation of the host dunite (Jousselin and Mainprice, 1998). Their modal composition is very variable, and they sometimes grade from dunite with 2-15% plagioclase to troctolites, and layered gabbros within few centimeters or few meters (Fig. 4b, see also Jousselin et al, 2012). More rarely, impregnated dunite contains euhedral plagioclase crystals (Fig. 4c), particularly in the MTZ between the Mahram outcrop and the Kl. lah outcrop. 25% of the logs contain cross-cutting ultramafic intrusions and concordant layers of the same composition in the lowermost crust; two of the intrusions are clearly rooted into the top of the MTZ. These intrusions have been well described and referred as "wehrlites" or "plagioclase wehrlites" in several studies (Benn et al, 1988; Juteau et al, 1988; Boudier and Nicolas, 1995; Jousselin and Nicolas, 2000b; Koga et al, 2001; Kaneko et al, 2014), which all point that they derive from the MTZ. The modal composition of three samples, and their similarity with samples from other studies is shown in Fig. 5; this shows that these rocks should not be called wehrlites in a strict sense. This is also pointed out by Kaneko et al (2014), who explain that they use the term "wehrlitic intrusion" in a "descriptive sense". At the sample scale, like for the MTZ, the composition can vary strongly within few meters or centimeters, and

ranges from dunite to olivine-rich troctolites, even gabbro, and very rarely wehrlite; in the Maqsad region, most of them contain >10 % plagioclase, and <5% clinopyroxene.

3.2.2. *New observations in the MTZ.*

At the base of the MTZ, we found seven outcrops of impregnated dunite with an isotropic fabric (Fig. 1 and 4d). This lithology has also been described before with the two examples of the Mahram outcrop (Boudier and Nicolas, 1995), and the Khilah outcrop (Jousselin et al, 2012). However, as we find more of them, we notice that they all are at the base of the MTZ, or very near the base. The isotropic outcrops are a few meters to 700 meters wide, with a thickness of a few meters, up to 50 meters. Two contain 20 cm wide planar vertical dunite veins devoid of impregnations, implying that melt has locally been extracted upward (Fig. 4e). The NW-SE strike of these veins is the same as that of the overlying sheeted dike complex. Another new finding is the occurrence of horizontal levels of stockwork-like magmatic breccias (Fig. 4d). Three were found at the top of the MTZ, while five others occur at the base of the MTZ, with two of these overlying and in continuity with isotropic impregnations in depleted harzburgite. None are found in the MTZ mid-section. The breccias consist of webs of centimeter-scale gabbro veins, encasing pluri-centimetric blocks of dunite (Fig. 4f). In three cases (Mahram, 110A69, 110A76 logs in Fig. DR1), series of dikes are rooted in the breccias at the base of the MTZ. The dikes are several centimeters to one-meter thick, parallel to the crustal sheeted-dikes. In six out of the fifteen cross-sections, the base of the crustal section shows steeply dipping gabbro layers that are at high angles to the subhorizontal Moho (Fig. 4g). Similarly, discordance of dunite foliations had been observed in one cross-section (figure 7e in Jousselin et al, 1998), suggesting that rigid blocks, separated by melt rich zones, had been rotated with respect to another, as magmatic breccias do at the centimetric scale. Observation of the gabbro-peridotite interface does not show any evidence of a shear zone, or of plastic or brittle deformation, and the lateral continuity of this interface is irregular (Fig. 4h) unlike for a planar faulted contact.

4. DISCUSSION

The MTZ is the deepest site where melt accumulates and starts crystallization. How the MTZ develops, how far it extends, how melt circulates inside, may play a role in the accretion of the crust above. Our most important, and surprising result is to find areas with a thin MTZ above the core of the Maqsad diapir, as mantle diapirs are always associated with a thick MTZ. This finding, coupled with few new observations lead us to propose a model for the formation of the MTZ. We then examine what should be observed at sea if the same processes are active, and discuss if current geophysical observations fit with the model.

4.1. Melt accumulation, and dunite formation at the base of the MTZ

The outcrops with isotropic impregnations from melt are only found at the base of the MTZ, beneath pure dunite, and partly hosted by depleted harzburgite. The fact that the mantle anisotropic plastic fabric was obliterated implies that the solid connection between grains was lost, thus enough melt accumulated in-situ to reach the critical fraction ($\approx 30\text{-}40\%$; Van der Molen and Paterson, 1979), which marks the transition from impregnated solid to suspension flow. Olivine grains coated with films of plagioclase illustrate the loss of the olivine grain interconnection (Fig. 4c). Also the presence of euhedral plagioclase within impregnated dunite (Fig. 4d) shows that crystals grew in suspension before melt extraction. The location and the restricted extension of such outcrops suggest that each derives from a single melt pulse, which stopped beneath the base of the MTZ. As shown by several studies (Boudier and Nicolas; 1995; Koga et al, 2001), most of the dunite is a product of melt/rock reaction where orthopyroxene of the host harzburgite is dissolved. With the harzburgite bordering the outcrops, and the presence of orthopyroxene relics in one of the outcrops with isotropic impregnations (the Mahram outcrop), we infer that the accumulated melt transforms the shallowest harzburgite into dunite, thus making the MTZ thicker.

4.2. What stops melt ascent at the base of the MTZ?

It is unclear why melts stop and accumulate at the base of the MTZ, rather than rise through the MTZ. We infer that the base of the MTZ may act as a barrier for at least a portion of the rising melt, and propose possible mechanisms depending on the mode of melt transport. The question of whether melt is transported in hydrofractures (Nicolas, 1986, Richardson, 1998, Klaessens et al, 2021) or in porous-flow channels (Kelemen et al, 1995) remains controversial. In the MTZ itself, we observe dikes and impregnations, which suggest that both processes could be active, but we cannot present clear-cut evidence for what happens further beneath.

In the case of dikes propagation, it can be arrested by several factors (Dahm, 2000; Gudmunson and Brenner, 2001), including discontinuities such as a bedding surface or a pre-existing fracture, changes in the host rock stiffness, and stress barriers. The contrast in Young's modulus, which quantifies the relationship between stress and strain in elastic materials, between harzburgite and the MTZ is unknown and largely depends on the melt fraction that could already be present at the base of the MTZ; if the MTZ is a soft layer in extension, it is conceivable that it acts as a boundary, impeding the propagation of fluid-filled fractures (Gudmunson and Brenner, 2001).

In the case of porous flow models, it is assumed that melt can circulate along grain boundaries in a way similar to a liquid flowing through a porous media, following Darcy's law (e.g. Ahern and Turcotte, 1979). However, peridotites do not contain open pores as sedimentary rocks do; some space has first to be created for melt to infiltrate the olivine matrix. This constraint is illustrated in the setup of experimental work by Pec et al (2015), in which a sample already containing melt-filled space has to be placed between a melt source and a melt sink to investigate

melt migration. The melt would not migrate from the source to the sink without the built-in presence of melt in between, giving the needed pore-space, and allowing transmission of a pressure gradient to drive melt flow. This constraint may be released in harzburgite as Daines and Kohlstedt (1994) have shown that the presence of orthopyroxene may operate as a sink for orthopyroxene-undersaturated melt. In this case, the chemical disequilibrium between melt and harzburgite can drive melt flow, and the dissolution of orthopyroxene could provide the needed melt-filled space for the reacting-melt progression, although it is possible that local volume increase needed for orthopyroxene melting, may be impeded by the lithostatic pressure. On the other hand, at the base of the MTZ, if orthopyroxene is not present, or if an earlier melt does not wet grain boundaries, offering a ready-made porosity network, melt cannot benefit from any available space to progress. With olivine dissolution being nonexistent or negligible (Kelemen et al, 1995), the dunite grain boundaries may be sealed and hinder "porous" migration of melt.

Once melt stops beneath the lowermost dunite, it reacts with the host harzburgite and transforms it into dunite. Once this dunite is compacted and melt-free, it could, in turn, stop the next melt pulse. If a dunite barrier is needed to stop rising melt and form new dunite, how does the first layer of dunite form? A possibility is that dunite produced in the rising mantle may have reached the Moho. Another possibility is that the uppermost dunite has a cumulate origin (Abily and Ceuleneer, 2012). An alternative proposition is that it was produced as a reaction zone at the base of the crust, similar to dunite produced by reaction around melt-filled hydrofractures, as found along coarse-grained gabbro dikes in the harzburgite (Boudier and Nicolas, 1977; Morgan and Liang, 2003). Whenever melt is in contact with harzburgite, a reaction zone in which orthopyroxene is dissolved, is formed. Magma at the base of the crust must incite the same dunite-forming reaction. In this case, the presence of magma responsible for the reaction front is continuous in time, unlike for a short-lived dike. If the reaction front beneath the Moho progresses

faster than the harzburgite rises from below, several meters of dunite may form over time. Reacting dikes in the harzburgite give a rough estimate of how fast a dunite reaction zone grows: they bear dunite rims that are several centimeters wide, and formed within the lifetime of the dike, possibly a few weeks to a year if it fits the duration of a magmatic event (e.g. Embly et al, 1995, Buck et al, 2006). This observation suggests that, wherever the lowermost gabbros contain some melt, several tens of centimeters of dunite per year may be formed by this reaction, with a reaction front moving downward from the Moho. Assuming that mantle flow velocity is of the same order as plate spreading (≈ 10 cm/year), the dunite should flow away at a slower velocity than the progression of the dunitization front. Thus, over time, a dunite reaction zone, a few meters thick, should form beneath the Moho. Interestingly, the slight increase downward in olivine Mg# and nickel content, and decrease in TiO₂ content in chromite-spinel, found at the top of one section of the Maqsad MTZ by Abily and Ceuleneer (2012), are similar to trends observed in the smaller scale reaction zone produced in the experiment of Morgan and Liang (2003), in which harzburgite is juxtaposed with the overlying basaltic melt.

4.3. Melt transfer from the base of the MTZ to the base of the crust

The outcrops with isotropic impregnations must represent a transient stage of melt emplacement. Their position near the apex of the diapir, close to the ridge axis, may explain why some are preserved and are not strongly affected by the diverging ridge flow. When they are not fossilized in this stage, they must endure plastic flow of the host mantle. Indeed, the Khilah outcrop shows external parts of the outcrop that are partially, tectonically transposed (Jousselin et al, 2012). Melt accumulation, its compaction due to mantle flow, and possible melt volume increase due to the dissolution of orthopyroxene in the host harzburgite, should induce fluid overpressure. This can explain the formation of the melt breccia and dikes (Fig. 4f) that are found near the base of the MTZ, sometimes in continuity with the isotropic impregnations. When the overpressure is enough,

the hydrofracturing dikes may breach through the horizontal dunite barrier that had temporarily stopped the melt migration, and brought melt to the base of the crust. When the melt is extracted, it leaves planar zones of melt-free dunite in the mush zone (Fig. 4e). In the end, melt extraction is not always complete; remaining melt forms impregnations, and gabbro lenses in the dunite, which are progressively transposed by mantle flow (Jousselin and Mainprice, 1998; Jousselin et al, 2012). We have seen that layered gabbro at the base of the crust, that are usually horizontal and parallel to the Moho, can be rotated at a steep angle with the Moho (Fig. 4g,h). However, no fault is observed at the peridotite-gabbro contact, and the gabbro is not affected by plastic nor brittle deformation; this deformation occurred in the magmatic state, and while the gabbros were not crystallized, during ridge accretion. We propose that when batches of magma reach the top of the MTZ, they form an unstable floor for the partially molten crust at the ridge axis, allowing slide and tilt of gabbro blocks, and causing the formation of the discordant structures.

4.4. How much melt is needed to form the MTZ?

It is difficult to precisely estimate how much melt is needed to dissolve pyroxene over the extent of the MTZ thickness. It depends on the melt composition, the time of residence for the melt, and whether melt is distributed along grain boundaries and forms a melt-rock intimate mixture, or is distributed in dikes and sills. While investigating the reaction stoichiometry, Kelemen (1990) calculated that 40 g harzburgite with 30 wt. % enstatite needs 60 g liquid saturated in Forsterite + Anorthite to form 37g Forsterite + 63 g liquid. This suggests that in a closed system, with a harzburgite density of 3.2 g/cm^3 and liquid density of 2.7 g/cm^3 , 64% melt volume is required to transform harzburgite into dunite; and with a forsterite density of 3.27 g/cm^3 , one volume of dunite is associated to two volumes of melt that participated to its formation. In an open system such as the MTZ, the melt fraction could be less at any given time. Also, Oman harzburgites often have a lower 20-25 % orthopyroxene content (e.g. Godard et al, 2000), which

should require less melt to dissolve. These considerations suggest that the 300-450 m maximum thickness of the MTZ beneath the Maqsad diapir formed by interaction with the equivalent in thickness of about 600 to 900 m of liquid. Comparison with the 5-6 km thick crust above the diapir suggests that, to first order, only ≈ 10 to 15 % fraction of the melt represented by the crust is needed to build the MTZ. As this fraction of the melt may be less undersaturated in orthopyroxene than the rest of the crust, this process may explain the presence of orthopyroxene as a minor cumulus phase in layered gabbros recovered at Hess-Deep (Gillis et al, 2013). What happened with the rest of the melt is unclear; we can only speculate that parts of it may have stagnated with the reacting melt in places where orthopyroxene was already dissolved or that it did not stop at the base of the MTZ because conditions for the melt to stop were not fulfilled.

4.5 The MTZ thickness reduction away from diapirs: tectonic thinning and intrusion into the crust.

The MTZ thickness reduction has been addressed in earlier studies (Benn et al, 1988; Jousselin and Nicolas, 2000b), which we recall here. First, the MTZ is accreted over a limited region above the mantle diapir, and above the horizontal radial mantle flow at the outskirts of the diapir (Fig 1b); this implies that the MTZ thins when it is stretched over a wider surface as it spreads away from the diapir. Schematically, a 200 m thick MTZ over a 3.2 km radius is the same volume as a 20 m thick MTZ over a 10 km radius. Thus, as the MTZ spreads away from where it is accreted, the radial flow geometry imposes a tectonic thinning of the MTZ. Second, as was observed in previous studies, ultramafic intrusions in the lower crust are directly rooted in the top of the MTZ. While called "wehrlites" or "plagioclase wehrlite" as a generic term, in detail these intrusions are also described as dunites, mela-troctolites, troctolites, mela-olivine gabbros, and are fairly similar to impregnated facies of the MTZ (Juteau et al, 1988a; Benn et al, 1988; Boudier and Nicolas, 1995; Jousselin and Nicolas, 2000b; Koga et al, 2001; Kaneko et al, 2014). It was thus

proposed that the intrusions simply correspond to a mixture of melt with olivine dunite-xenocrysts and possibly few phenocrysts, formed in the MTZ, and squeezed into the overlying crust, thus participating in the MTZ thinning (Juteau et al, 1988a; Benn et al, 1988; Jousselin and Nicolas, 2000b). The chemistry of olivine, plagioclase and clinopyroxene in the intrusions is similar to that of the MTZ (Kaneko et al, 2014); the trace element compositions of their clinopyroxene also support the genetic link between the MTZ and the so-called "wehrlitic" intrusions, and record equilibrium with a MORB-type melt (Koga et al, 2001); this has led to associate these intrusions to the magmatic phase of the V1-Geotimes Unit, rather than a later depleted magmatism (Kaneko et al, 2014; Koga et al, 2001). The process of intruding parts of the MTZ into the crust is probably more important than tectonic thinning as it explains better the dramatic shift from a peak MTZ thickness to a thin one; it is also required to realistically balance the volume of the crustal ultramafic units with the production of the MTZ (Jousselin and Nicolas, 2000b).

Several forces have been involved to provide the pressure necessary to extrude MTZ material upward in the crust. Gabbro layers at the borders of the intrusions are deformed with folds, with ultramafic material penetrating into the layers, showing that the intrusion occurred when the gabbros were still hot and not fully crystallized. With these crosscutting relationships in mind, Juteau et al (1988a) and Kaneko et al (2014) consider that the intrusions are slightly late relative to the gabbro formation, and that the tectonic inversion during the ophiolite detachment from the spreading center may have helped the upward movement of magmatic mush in the MTZ. On the other hand, the lower gabbros contain concordant layers of the same ultramafic lithologies, deformed by magmatic flow, showing that they are contemporaneous with the magma chamber activity. Thus, the crosscutting intrusions may have been emplaced on the flanks of the magma chamber and preserved from tectonic transposition, while intrusions emplaced in the partially molten gabbro at the base of the crust were transposed into concordance with the gabbro layering.

In a model where the intrusions are formed during the crustal accretion process, Benn et al (1988) and Joussetin and Nicolas (2000b) propose that the driving force for squeezing weak parts of the MTZ into the crust is the horizontal forced mantle flow produced by diapirs at the spreading center.

For clarity, we point that not all the ultramafic intrusions in the lower crust have the same origin; clear distinctions are evidenced by Adachi and Miyashita, 2003 and Kaneko et al, 2014. Other intrusions that are true wehrlites, with stronger clinopyroxene content, are probably produced by adding water (possibly from the subducting slab beneath) to primitive MORB melts (Koepke et al, 2009). These rocks are always discordant with respect to gabbro layering. They are more common in the northern massifs, have distinct depleted mineral compositions, that differ from the MTZ; in particular their clinopyroxenes are characterized by very low Ti and Na contents, akin to those of the V2-Lasail Unit, suggesting that they belong to the later arc-like phase.

4.6. A synthetic model of MTZ accretion and thinning

Our model is synthesized in Fig. 6. Melt accumulates beneath melt-free dunite in the shallowest harzburgite. It reaches a fraction greater than 30% which leads to destroy the solid framework of the host peridotite (Fig 4d). As it reacts with the harzburgite, it forms dunite, which makes the MTZ thicker (Fig. 2). With greater melt fraction, and compaction linked to the lithostatic pressure and mantle flow, melt is overpressured, and forms melt breccias (Fig. 4f) that extract melt to the base of the crust. This episodic melt delivery may perturb the orientation of the crustal lowermost layered gabbros (Fig. 4g,h). Then the MTZ thickness is reduced because of tectonic thinning, and probably the injection of weak zones (melt loaded) of the MTZ into the crust.

4.7. Predictions for marine geophysical observations, and coherency with existing data.

In this section, we tentatively derive from our results and model some predictions for marine geophysical observations. By doing so, we assume that our observations and our model are related to the V1 magmatism, and that this phase of accretion is a good analog of processes at fast spreading ridges. We also gather marine geophysical observations that unveil features at the Moho and beneath the Moho at the fast spreading East Pacific Rise (Fig. 7) and discuss how they could be interpreted in light of our results. Our observations from the Oman ophiolite suggest that sub-Moho melt lenses should exist mainly (if not only) at the base of the MTZ near oceanic ridges. The thickening of the MTZ with distance from the axis seen in the ophiolite leads to predict that sub-Moho melt-lens reflectors should be observed off-axis, at increasing depth with distance from the rise. The melt lenses have a limited life span, as once emplaced at the base of the MTZ, melt is later expelled into the crust; thus reflectors may disappear and new ones may appear with time. Conversely, no reflectors deeper than the Moho should be found directly right beneath the axis. The mantle tomography study of Toczey et al (2007) provides an image of the last 4 km layer beneath the Moho; it cannot resolve the presence of a MTZ, but reveals the presence of several enhanced melt upwelling centers, approximately at 9°57'N, 9°43'N, 9°30'N, 9°15'N, 9°05'N, a more diffuse one at 8°57'N, and another at 8°30'N not shown in Fig. 7. Modeling shows that these anomalies could be consistent with the presence of Oman-like diapirs (Jousselin et al, 2003). The anomalies have a near 20-25 km spacing that matches the Oman diapir spacing. They nevertheless seem a bit wider (≈ 8 -10 km width) than the Oman diapirs, and this larger size may lead to a thicker MTZ extending further than 6 km from the ridge. Seismic rays with a vertical incidence through the MTZ should travel along the slow axis of the anisotropic horizontal dunite, with a seismic velocity on the order of $7.4 \text{ km/s} \pm 0.2\text{s}$ (Jousselin and Mainprice, 2000). With a <1 km thick MTZ, 5-10 km from the rise, this suggests that reflectors should be found 0.1-0.3 s (two-way

travel time) beneath the Moho. This result partly matches observations of sub-Moho reflectors by Barth et al (1991) at 0.2-0.4s beneath the Moho; the consistent dip towards the ridge of the most outward reflectors may correspond to the zone where the MTZ thins over a 1-3 km horizontal distance. Melt-rich zones found at greater distances, at or above the Moho (Crawford and Webb, 2002) are more probably related to the "wehrlite" (MTZ-like) intrusions in the crust, and may explain the surprising crustal thickening observed on the ridge flanks, 5 to 10 km from the ridge axis (fig 7d in Aghaei et al, 2014). The abrupt thinning of the MTZ suggests that no detectable trace of the MTZ should remain tens of kilometers away from the ridge. This fits the distribution of upper mantle reflections, which are found at 7.1 ± 3.2 km from the ridge, and not beyond (Barth and Mutter, 1991), while seismic lines extend well beyond this distance from the ridge. One incoherent observation, if we were to associate mantle diapirs with the strongest lows in the mantle low velocity zone (MLVZ) (Jousselin et al, 2003), is that upper mantle reflectors are not always strictly associated to the strongest lows in the MLVZ, and can be found in between these maxima (figure 7). Also, the mantle reflectors should be found on either side of the MLVZ. That is not the case between $9^{\circ}20'N$ and $9^{\circ}30'N$ where the MLVZ is 12 km off-axis, and two reflectors are ≈ 5 km apart from the ridge, west of the MLVZ, which is not centered on the ridge.

Another aspect of the seismic Moho at the EPR, is that it is sometimes absent, or has differing expressions (Kent et al, 1994; Aghaei et al, 2014). Thick MTZs are believed to generate a seismic diffusive Moho type, while thin MTZs would correspond to impulsive or shingled Moho types (Aghaei et al, 2014). While this is not clearly stated, this interpretation probably relies on the assumption that the MTZ is composed of thin alternating gabbro and dunite layers, where the ratio of dunite to gabbro gradually increases with depth (Nedimovic et al, 2005). This idealized view corresponds to descriptions of the very thick MTZ (up to 3 km) in the Bay of Islands ophiolite complex (Karson et al, 1984), but departs from our observations in Oman, and the log of Abily

and Ceuleneer (2012), where gabbro lenses are rare and <10 meters thick. Thus the correspondence between the seismic type of Moho and the MTZ thickness is unclear. If the top of the MTZ is mainly composed of dunite as in Oman, its seismic velocity is greater than the velocity of harzburgite, providing a stronger contrast with the crustal velocity, especially if the crust is devoid of wehrlitic injections; thus a thick MTZ could correspond to impulsive Moho types. This may explain why the 9°42'N-9°49.5'N region of the EPR, which is nearly centered on a MLVZ at 9°43'N, possibly corresponding to a mantle diapir, is associated with more strong and impulsive Moho reflections (Aghaei et al, 2014). Following previous studies (Benn et al, 1988; Joussetin and Nicolas, 2000), we associate troctolite-wehrlite intrusions in the crust to a strong compaction of the MTZ at the periphery of mantle diapirs. Accordingly, wehrlitic-rich, and olivine-rich gabbro units -with fast seismic velocities associated to the olivine- are particularly present in the crust at the periphery of mantle diapirs. Similar rocks, interpreted as intrusive rock or samples from the MTZ have been reported at the EPR and the Mid-Atlantic Ridge (Girardeau and Francheteau, 1993). This stratigraphy may produce a progressive velocity gradient from the lower crust to the crust-mantle interface, which would produce a diffuse Moho at the periphery of diapirs. We also found that some gabbro layers may be vertical just above the horizontal crust-mantle interface (Fig 4g, h). The consequence is that the fast velocity axis in the gabbro can be co-linear with reflected seismic ray incidence. The juxtaposition with a vertical slow axis in the mantle beneath may reduce the crust/mantle velocity contrast, and explain the absence of a seismic Moho, or produce a weak and diffuse Moho. This could be true for the diffuse Moho along 9°49.5'N-9°57'N, at the southern edge of the anomaly centered on 9°57'N, in an area which contains several off-axis melt lenses in the lower crust and a large one in the upper crust, and where plate loading by the Lamont seamounts causes a steeper than normal western ridge flank, with a 150 meters deep depression. These factors may cause significant deformation and upward block rotations of layered gabbros. Aghaei et al (2014) also suggest that melt source interactions between the ridge

and the Lamont seamounts may occur and affect the Moho. For sites of off-axis eruptions, away from the axial low velocity zone, we refer to the geology of an off-axis melt delivery zone (Jousselin and Nicolas, 2000a), which suggests a more complex structure.

5. SUMMARY AND CONCLUSION

The Oman ophiolite has preserved accretion centers that fed a fast spreading center; it provides a useful window into processes that occur at the crust-mantle boundary, which are complementary to marine geophysical data collected at currently active ridges. The Oman paleo-ridge is underlain by mantle diapirs, which are similar in size and spacing to those of velocity minima found in the mantle, 0-4 km beneath the Moho at the EPR (Toomey et al, 2007). The diapirs are capped by a Moho transition zone, mainly made of dunite (> 95%), which sometimes contains "melt" (plagioclase and clinopyroxene) impregnations, and layered gabbro lenses (less than 5% vol.). We found that the MTZ grows from a few meters thickness at the ridge, to a maximum 450 meters thickness approximately 6 kilometers from the ridge axis, and thins to a few meters in the next further 2 kilometers. Several outcrops of isotropic melt impregnation in dunite and depleted harzburgite are found, only at the base of the MTZ section. They suggest that locally, a fraction of melt, large enough to disconnect most crystal of the host rock, accumulated in a time frame small enough that strain related to the host mantle flow was not recorded by the magmatic mush. They also suggest that the base of the MTZ acts as a barrier for some of the melt rising from below. We propose that the presence of harzburgite, which contains orthopyroxene that can be dissolved by melt, helps melt migration, while dunite of the MTZ could be hard to penetrate for melt if grain boundaries are not opened with melt already present. This suggests that dunite could transport melt only when it is being formed, not after it is compacted (dunite offers a "single ride" as a porous matrix). However, further investigations are certainly needed to understand why melt stops and accumulates at the base of the MTZ. Once melt is ponding at this barrier, it dissolves the

remaining orthopyroxene of the uppermost harzburgite, thus forming new dunite. Compaction leads to melt overpressure and formation of melt breccia and dikes that can extract the melt upward. This suggests to a model, in which successive pulses of magmatic underplating, and interaction with the host harzburgite, thicken the MTZ as it drifts away from the ridge axis. The model predicts that magma lenses should be found only at the Moho when beneath the ridge, and at growing depth with increasing distance from the ridge. Depending on the size of the melt delivery zone (up to 6 km away from the ridge axis in Oman, maybe up to 10 km at the EPR), the melt lenses could be found at depths of 0.5-1 km. Once further away, melt lenses should be found in the lower crust only (not beneath the Moho), and should correspond to bits of the MTZ expelled upward, forming so-called wehrlitic intrusions that significantly thicken the crust. These predictions seem broadly coherent with the distribution of sub-Moho seismic reflectors at the EPR, crustal-thickening within 7 kilometers from the ridge, and provide tentative explanations for the different types of Moho unveiled by marine geophysical experiments, which are different from those derived from the MTZ structure described in the Bay of Island ophiolite.

ACKNOWLEDGMENTS

This study was financially supported by the Institut National des Sciences de l'Univers (INSU-CNRS) through its SYSTÈM program. We are grateful to Alexandre Flammang (Otelo, Université de Lorraine) and Christophe Nevado (Géosciences Montpellier) for the polished thin sections, and the Directory of Minerals at the Ministry of Commerce and Industry of the Sultanate of Oman for their hospitality. We thank J. R. Deans, J. Koepke and an anonymous reviewer for their comprehensive comments that helped to clarify the manuscript, and J. Koepke and P. Agard for editorial handling

REFERENCES CITED.

- Abily, B., and Ceuleneer, G., 2012, The dunitic mantle-crust transition zone in the Oman ophiolite: residue of melt-rock interaction, cumulate from high MgO melts, or both? *Geology*, V. 41(1), p. 67-70, doi:10.1130/G33351.1.
- Adachi, Y. and Miyashita, S., 2003, Geology and petrology of the plutonic complexes in the Wadi Fizh area: Multiple magmatic events and segment structure in the northern Oman ophiolite, *Geochem. Geophys. Geosyst.*, 4(9), 8619, doi:10.1029/2001GC000272.
- Aghaei, O., Nedimović M.R., Carton H., Carbotte S.M., Canales J.P., and Mutter J.C., 2014, t from 9°42'N to 9°57'N from poststack-migrated 3D MCS data *Geochem. Geophys. Geosyst.*, v. 15, p. 634–657, doi:10.1002/2013GC005069.
- Ahern, J.L. and Turcotte, D.L., 1979. Magma migration beneath an ocean ridge. *Earth and Planetary Science Letters*, v. 45, p. 115-122, [https://doi.org/10.1016/0012-821X\(79\)90113-4](https://doi.org/10.1016/0012-821X(79)90113-4).
- Akizawa, N. and Arai, S., 2009, Petrologic profile of peridotite layers under a possible Moho in the Northern Oman ophiolite: an example from Wadi Fizh, *Journal of Min. and Petrol. Sciences*, v. 104, p. 389-394.
- Alabaster, T., Pearce, J.A., Malpas J., 1982. The volcanic stratigraphy and petrogenesis of the Oman ophiolite complex. *Contrib. Mineral. Petrol.*, v81, p. 168-183.
- Barth, G.A., Mutter, J.C., and Madsen, J.A., 1991, Upper-mantle seismic reflections beneath the East Pacific Rise, *Geology*, v. 19, p. 994-996, doi:10.1130/0091-7613(1991).
- Belgrano, T. M., and Diamond, L. W. , 2019, Subduction-zone contributions to axial volcanism in the Oman-U.A.E. ophiolite, *Lithosphere*, 11(3), 399–411, <https://doi.org/10.1130/L1045.1>
- Benn, K., Nicolas, A. and Reuber, I., 1988, Mantle-crust transition zone and origin of wehrlitic magmas: Evidence from the Oman ophiolite, *Tectonophysics* v. 151, p. 75–85, [doi:10.1016/0040-1951\(88\)90241-7](https://doi.org/10.1016/0040-1951(88)90241-7).
- Boudier, F. and Nicolas, A., 1977, Structural control on the partial melting of the Lanzo peridotite. Magma genesis: AGU Chapman Conf. Proc. on Partial melting in the Earth's upper mantle, Dick

- H.J.B. (ed), Oregon Dep. Geol. Min. Industries, Bull. v. 96, p. 39-56.
- Boudier, F., Ceuleneer, G., and Nicolas, A., 1988, Shear zones, thrusts and related magmatism in the Oman ophiolite: initiation of thrusting on an oceanic ridge, *Tectonophysics*, v. 151, p. 275-296.
- Boudier, F. and Nicolas, A., 1995, Nature of the Moho transition zone in the Oman ophiolite, *Journal of Petrology* v. 36, p. 777-796, doi:10.1093/petrology/36.3.777.
- Boudier, F., Nicolas, A., Ildefonse B. and Jousset, D., 1997, EPR microplates, a model for the Oman ophiolite, *Terra Nova*, v. 9, p. 79-82, doi:10.1111/j.1365-3121.1997.tb00007.x.
- Buck, W. R., P. Einarsson, and B. Brandsdóttir, 2006, Tectonic stress and magma chamber size as controls on dike propagation: Constraints from the 1975–1984 Krafla rifting episode, *J. Geophys. Res.*, 111, B12404, doi:10.1029/2005JB003879
- Carbotte, S.M., Marjanovic M., Carton H., Mutter J.C., Canales J.P., Nedimović M.R., Han S., and Perfit M.R., 2013, Fine-scale segmentation of the crustal magma reservoir beneath the East Pacific Rise, *Nature Geoscience*, v. 6, p. 866-870.
- Crawford W. and Webb, S.C., 2002, Variations in the distribution of magma in the lower crust and at the Moho beneath the East Pacific Rise at 9°-10°N, *Earth and Planetary Science Letters*, v. 203, p. 117-130, doi:10.1016/S0012-821X(02)00831-2.
- Dahm, T., 2000, Numerical simulations of the propagation path and the arrest of fluid-filled fractures in the Earth, *Geophys. J. Int.*, v. 141, p. 623-638.
- Daines M.J., and Kohlstedt, D.L., 1994, The transition from porous to channelized flow due to melt/rock reaction during melt migration, *Geophysical Research Letters*, v. 21(2), p. 145-148.
- Embley, R. W., W. W. Chadwick Jr., I. R. Jonasson, D. A. Butterfield, and E. T. Baker, 1995, Initial results of a rapid response to the 1993 CoAxial event: Relationships between hydrothermal and volcanic processes, *Geophys. Res. Lett.*, v. 22(2), p. 143–146.
- Ernewein, M., Pflumio, C. and Whitechurch, H., 1988. The death of an accretion zone as evidenced by the magmatic history of the Sumail ophiolite (Oman), *Tectonophysics*, v. 151, p.

247–274, [http://dx.doi.org/10.1016/0040-1951\(88\)90248-X](http://dx.doi.org/10.1016/0040-1951(88)90248-X).

Gillis K.M., Snow, J.E., et al., 2014, Primitive layered gabbros from fast-spreading lower oceanic crust, *Nature*, v. 505, p. 204-207, doi:10.1038/nature12778.

Girardeau, J. and Francheteau, J., 1993, Plagioclase-wehrlites and peridotites on the East Pacific Rise (Hess Deep) and the Mid-Atlantic Ridge (DSDP site 334): evidence for magma percolation in the oceanic upper mantle, *Earth and Planetary Science Letters*, v. 115, p. 137–149.

Godard, M., Jousselin, D., and Bodinier, J.L., 2000, Relationships between geochemistry and structure beneath a palaeo-spreading centre: a study of the mantle section in the Oman ophiolite, *Earth and Planetary Science Letters*, v. 180, p. 133-148, doi: [10.1016/S0012-821X\(00\)00149-7](https://doi.org/10.1016/S0012-821X(00)00149-7).

Godard, M., Bosch, D., Einaudi, F., 2006, A MORB source for low-Ti magmatism in the Semail ophiolite, *Chem. Geol.*, v. 234, p. 58-78. doi.org/10.1016/j.chemgeo.2006.04.005.

Gudmundsson, A. and Brenner, S.L., 2001, How hydrofractures become arrested, *Terra Nova*, v. 13, p. 456-462.

Guilmette, C., Smit, M.A., van Hinsbergen D.J.J., Gürer, D., Corfu F., Charette B., Maffione M., Rabeau O. and D. Savard, 2018, Forced subduction initiation recorded in the sole and crust of the Semail Ophiolite of Oman, *Nature Geoscience*, V11, p. 688-695.

Hacker, B.R., 1994, Rapid emplacement of young oceanic lithosphere: argon geochronology of the Oman ophiolite, *Science*, V. 265, p. 1563-1565.

Ildefonse, B., Billiau, S. and Nicolas, A., 1995, A detailed study of mantle flow away from diapirs in the Oman ophiolite. In R. L. M. Vissers and A. Nicolas (eds), *Mantle and Lower Crust Exposed in Oceanic Ridges and in Ophiolites*, Kluwer Academic Publishers, Dordrecht, pp. 163–177.

Jousselin, D., Nicolas, A. and Boudier, F., 1998, Detailed mapping of a mantle diapir below a paleo-spreading center in the Oman ophiolite, *Journal of Geophysical Research*, v. 103, p. 18153-18170, doi:10.1029/98JB01493.

Jousselin, D. and Mainprice D., 1998, Melt topology and seismic anisotropy in the mantle

peridotites of the Oman ophiolite, *Earth and Planetary Science Letters*, v. 164, p. 553-568,

[doi:10.1016/S0012-821X\(98\)00235-0](https://doi.org/10.1016/S0012-821X(98)00235-0).

Jousselin, D. and Nicolas, A., 2000a, Oceanic ridge off-axis deep structure in the Mansah region (Sumail massif, Oman ophiolite), *Marine Geophysical Researches*, v. 21, p. 243-257, doi: DOI: 10.1023/A:1026741208295.

Jousselin, D. and Nicolas, A., 2000b, The Moho transition zone in the Oman ophiolite-relation with wehrlites in the crust and dunites in the mantle, *Marine Geophysical Researches*, v. 21, p. 229-241, doi:10.1023/A:1026733019682.

Jousselin, D., Dunn, R., and Toomey, D.R., 2003, Modeling the seismic signature of structural data from the Oman ophiolite: can a mantle diapir be detected beneath the East Pacific Rise? *Geochem. Geophys. Geosyst.*, v. 4(7), 8610, doi: 10.1029/2002GC000418.

Jousselin, D., Morales, L.F.G., Nicolle, M. and Sempant, A., 2012, Gabbro layering induced by simple shear in the Oman ophiolite Moho transition zone, *Earth and Planetary Science Letters*, v. 331-332, p. 55-66.

Juteau, T., Ernewein, M., Reuber, J., Whitechurch H., and Dahl R., 1988, Duality of magmatism in the plutonic sequence of the Sumail nappe, Oman, *Tectonophysics*, v. 151, p. 107-135.

Kaneko, R., Adachi, Y., and Miyashita, S., 2014, Origin of large wehrlitic intrusions from the Wadi Barghah to Salah area in the northern Oman ophiolite, *Geol. Soc. London, Sp. Pub.*, v. 392, p. 213-228, doi:10.1144/SP392.11.

Karson, J.A., Collins, J.A., Casey J., 1984, Geologic and seismic velocity structure of the crust/mantle transition in the Bay of Islands ophiolite complex, *Journal of Geophysical Research*, 89, 6126–6138, doi:10.1029/JB089iB07p06126.

Kelemen, P.B., 1990, Reaction between ultramafic rock and fractionating basaltic magma I. phase relations, the origin of calc-alkaline magma series, and the formation of discordant dunite, *J. of Petrol.*, v. 31, p. 51-98.

- Kelemen, P.B., Shimizu, N., and Salters, V.J.M., 1995, Extraction of mid-ocean-ridge basalt from the upwelling mantle by focused flow of melt in dunite channels, *Nature*, v. 375, p. 747-753.
- Kent, G.M., Harding A.J., and Orcutt J.A., 1993, Distribution of magma beneath the East Pacific Rise between the Clipperton transform and the 9°17'N deval from forward modeling of common depth point data, *J. Geophys. Res.*, v. 98, p. 13,945–13,969.
- Kent, G.M., Harding, A.J., Orcutt, J.A., Detrick, R.S., Mutter, J.C., Buhl, P., 1994, Uniform accretion of oceanic crust south of the Garrett Transform at 14°15'S on the East Pacific Rise. *Journal of Geophysical Research* v. 99, p. 9,097–9,116.
- Klaessens, D., Reisberg, L., Joussetin, D., Godard, M., and Aupart C., 2021, Osmium isotope evidence for rapid melt migration towards the Moho in the Oman ophiolite, *Earth and Planetary Science Letters*, V. 572, 117111, <https://doi.org/10.1016/j.epsl.2021.117111>
- Koepke, J., S. Schoenborn, M. Oelze, H. Wittrann, S. T. Feig, E. Hellebrand, F. Boudier, and R. Schoenberg, 2009, Petrogenesis of crustal wehrlites in the Oman ophiolite: Experiments and natural rocks, *Geochem. Geophys. Geolyst.*, 10, Q10002, doi:10.1029/2009GC002488.
- Koga, K.T., Kelemen, P.B. and Shimizu, N., 2001, Petrogenesis of the crust-mantle transition zone and the origin of lower crustal wehrlite in the Oman ophiolite, *Geochemistry-Geophysics-Geosystems*, v. 2, 1038, doi:10.1029/2000GC000132.
- MacLeod, C.J., Lissenberg, L. and Bibby, L. E., 2013, “Moist MORB” axial magmatism in the Oman Ophiolite: the evidence against a mid-ocean ridge origin, *Geology* 41, 459–462.
- Marjanovic, M., Carton, H., Carbotte, S.M., Nedimovic, M.R., Mutter, J.C., and Canales, J.P., 2015, Distribution of melt along the East Pacific Rise from 9°30' to 10°N from an amplitude variation with angle of incidence (AVA) technique, *Geophysical Journal International*, V203-1., p. 1-21. <https://doi.org/10.1093/gji/ggv251>.
- Ministry of Petroleum and Minerals of Sultanate of Oman, 1986 and 1987, Geological Map of Oman, scale 1:100 000.

- Morgan, Z., and Y. Liang, 2003, An experimental and numerical study of the kinetics of harzburgite reactive dissolution with applications to dunite dike formation, *Earth and Planetary Science Letters*, v. 214, p. 59–74.
- Nedimovic, M., Carbotte, S., Harding, A., Detrick, R., Canales, J.P., Diebold, J., Kent, G., Tisher, M., J. Babcock, 2005, Frozen magma lenses below the oceanic crust, *Nature*, 436, 1149-1152.
- Nadimi, A., 2002, Mantle flow patterns at the Neyriz Paleo-spreading center, Iran, *Earth and Planetary Science Letters*, v. 203, p. 93–104.
- Nicolas, A., and J.F. Violette, 1982, Mantle flow at oceanic spreading centers: Models derived from ophiolites, *Tectonophysics*, v. 81, p. 319-339.
- Nicolas, A., Prinzhofer, A., 1983. Cumulative or residual origin for the transition zone in ophiolites: structural evidence, *J. Petrol.*, v. 24, p. 188-206.
- Nicolas, A., 1986, A melt extraction model based on structural studies in mantle peridotites, *Journal of petrology*, 27, 999–1022, doi: 10.1093/petrology/27.4.999.
- Nicolas, A., Ceuleneer, G., Boudier, F., and Misseri, M., 1988, Structural mapping in the Oman ophiolites: mantle diapirism along an oceanic ridge, *Tectonophysics*, v. 151, p. 27-56.
- Nicolas, A., Boudier, F. and Ildefonse, B., 1994, Evidence from the Oman ophiolite for active mantle upwelling beneath a fast spreading ridge, *Nature*, v. 370, p. 51-53.
- Nicolas, A., and Boudier, F., 1995, Mapping oceanic ridge segments in Oman ophiolite, *J. Geophys. Res.* v. 100(B4), p. 6179-6197.
- Nicolas, A., Boudier, F. and Ildefonse, B., 1996, Variable crustal thickness in the Oman ophiolite: Implication for oceanic crust, *J. Geophys. Res.* 101: 17941–17950.
- Nicolas, A., and Boudier, F., 2015a, Structural contribution from the Oman ophiolite to processes of crustal accretion at the East Pacific Rise, *Terra Nova*, v. 27, p. 77-96, doi: 10.1111/ter.12137.
- Nicolas, A., and Boudier, F., 2015b, Inside the magma chamber of a dying ridge segment in the Oman ophiolite, *Terra Nova*, v. 27, p. 69-76, doi: 10.1111/ter.12130

- Nicolle, M., Jousselin, D., Reisberg, L., Bosch D., and Stephant, A., 2016, Major and trace element and Sr and Nd isotopic results from mantle diapirs in the Oman ophiolite: implications for off-axis magmatic processes, *Earth and Planetary Science Letters*, v. 437, p. 138–149, doi: [10.1016/j.epsl.2015.12.005](https://doi.org/10.1016/j.epsl.2015.12.005).
- Pec, M., Holtzman, B.K., Zimmerman, M., and Kohlstedt, D.L., 2015, Reaction infiltration instabilities in experiments on partially molten mantle rocks, *Geology*, v.43, p. 575-578, doi: [10.1130/G36611.1](https://doi.org/10.1130/G36611.1).
- Richardson, C.N., 1998, Melt flow in a variable viscosity matrix, *Geophysical Research Letters*, V27, n7, p. 1099-1102.
- Rioux, M., Browning, S., Kelemen, P., Gordon, S., Dudas, F., and Miller, R., 2012, Rapid crustal accretion and magma assimilation in the Oman- U.A.E. ophiolite: High precision U- Pb zircon geochronology of the gabbroic crust. *J. Geophys. Res.* v. 117, B07201, doi:10.1029/2012JB009273.
- Small, C., 1994, A global analysis of mid-ocean ridge axial topography, *Geophys. J. Int.*, v. 116, p. 64-84.
- Taylor, B., Zellmer, K., Martinez, F. and Goodliffe A., 1996, Sea-floor spreading in the Lau back-arc basin, *Earth and Planetary Science Letters*, v. 144, p. 35-40.
- Taylor, B. and Martinez, F., 2003, Back-arc basin basalt systematics, *Earth and Planetary Science Letters*, v. 210, p. 481-497, doi:10.1016/S0012-821X(03)00167-5
- Toomey, R.T., Jousselin, D., Dunn, R.A., Wilcock, W.S.D. and Detrick, R.S., 2007, Skew of mantle upwelling beneath the East Pacific Rise governs segmentation, *Nature*, v. 446, p. 409-414, doi:10.1038/nature05679.
- Van der Molen I. and Paterson, M.S., 1979, Experimental deformation of partially-melted granite. *Contributions to Mineralogy and Petrology*, v. 70, p. 299-318, doi: [10.1007/BF00375359](https://doi.org/10.1007/BF00375359).
- Warren, C.J., Parrish, R.R., Waters, D.J. and Searle, M.P., Dating the geologic history of Oman's

Semail ophiolite: insights from U-Pb geochronology", 2005, *Contrib. Mineral Petrol.*, 150, p. 403-422, doi:10.1007/s00410-005-0028-5.

Xu, M., Canales, J.P., Carbotte, S.M., Carton, H., Nedimovic, M.R., and Mutter, J.C., 2014, Variations in axial magma lens properties along the East Pacific Rise (9°30'N-10°00'N) from swath 3-D seismic imaging and 1-D waveform inversion, *J. Geophys. Res.*, v. 119, p. 2721-2744, doi:10.1002/2013JB010730.

FIGURE CAPTIONS

Figure 1. Geological setting; a) simplified map of dike distribution throughout the southern massifs of the Oman ophiolite; it also shows the emplacement-related low temperature deformation and the asthenospheric deformation preserved in the mantle section (adapted from Boudier et al, 1997). b) MTZ thickness distribution (39 thickness measurements in meters, boxes correspond to thicknesses constrained by logs, dark boxes correspond to logs shown in Fig. 3), and simplified lineation map of the Maqsad mantle diapir, showing in particular that mantle lineations striking parallel to the sheeted dike orientations are confined to a <2 km NW-SE corridor taken as the ridge axis (thick dashed line).

Figure 2. Graph of MTZ thickness as a function of distance from the ridge axis. MTZ thickness increases from a minimum value at the axis to a maximum ≈ 6 km from the axis, followed by a drastic reduction at greater distances; error range shown in lighter shade. As thick MTZs are associated to the presence of a mantle diapir beneath, it is well established that at any further distance from this structure, the MTZ remains thin (Nicolas et al, 1996).

Figure 3. Six examples of logs in the MTZ section (locations in Fig. 1), organized from left to

right with increasing distance from the ridge axis. Isotropic impregnation outcrops are found only at the base of the MTZ, while magmatic breccia outcrop at the base and/or the top of the MTZ. (4 c-h refer to illustrations in Fig. 4).

Figure 4. Field observations in the MTZ: (a) impregnated dunite with orthopyroxene grains relics in thin section (white: olivine with dashed lines as subgrains boundaries; light grey: orthopyroxene with exsolution lamellae when visible; darker grey: altered impregnating clinopyroxene; black: spinel grains); (b) segregated and transposed plagioclase impregnations in dunite, grading into olivine-rich gabbro lenses (c) euhedral plagioclase crystal in melt impregnated dunite/troctolite in the MTZ; (d) isotropic melt impregnation typical of those found at seven sites at the base of the MTZ; (e) planar vertical dunite zone void of isotropic impregnation; (f) Magmatic breccia with clasts of dunite; (g) view of a near horizontal crust/mantle contact with gabbro layers at a high angle with the contact (≈ 50 m high view); (h) close up view of a contact between layered gabbros at the base of the crust, and dunite at the top of the MTZ; gabbro layers are at a high angle with the irregular contact which is not faulted.

Figure 5. Modal compositions of samples from our study and others that have been referred as wehrlite, wehrlitic intrusions, and plagioclase-wehrlite.

Figure 6. Model of MTZ accretion. As the MTZ grows from left to right with time, it also drifts away from the axis. (a-b) Because non-impregnated dunite forms a dam for rising melt, melt accumulates beneath the base of the MTZ until the harzburgite solid framework is destroyed forming a texture of isotropic melt impregnation. At the same time, orthopyroxene is dissolved and the harzburgite is transformed into dunite, thus thickening the MTZ. (c-d) Melt is overpressured and forms magmatic breccia and dikes able to break through the overlying dunite

barrier; as melt reaches the crust, new breccia may form; this weak-unstable basement may be the cause of perturbations and rotations of modal layering and magmatic flow structures in the overlying partially molten crust. (e) Plastic flow in the mantle and magmatic flow in the crust progressively erase features produced during stages a-d; this process is repeated as new melt pulses are delivered as long as the MTZ is above the 12 km wide melt delivery zone. (f) Tectonic thinning, and intrusion of bits of the MTZ into the crust reduce the MTZ thickness.

Figure 7. Compilation of pertaining marine geophysical data from 8°50'N to 10°N, at the East Pacific Rise (solid line), with contours from the mantle low velocity zone from Toomey et al, 2007 (7.5 km/s; 7.4 km/s; 7.3 km/s), seismic lines (grey lines) with sub-Moho reflectors (thick nail-like bars) from Barth et al, 1991, and color coded diffusive (D), shingled (S), and impulsive (I) Moho from Aghai et al, 2014.

SUPPLEMENTAL INFORMATION

Transect locations / locations of photographs in Fig. 4

15 precise transects were logged (figure DR1a); each is associated to a field station (figure DR1b) as follow

-96OD74

base of MTZ: 23°07.879'N; 57°55.5974'E; 700 m

summit of MTZ: 23°07.686'N; 57°56.219'E; 900 m

-110A69

base of MTZ: 23°06.249'N; 57°56.595'E; 910 m

summit of MTZ: 23°06.447'N; 57°56.728'E; 1040 m

-110A76

base of MTZ: 23°06.205'N; 57°56.78'E; 900 m

summit of MTZ: 23°06.445'N; 57°56.97'E; 1050 m

-13OD13

base of MTZ: 23°01.761'N; 58°0.003'E; 725

summit of MTZ: 23°02.484'N; 58°00.295'E; 850 m

-Mahram outcrop

base of MTZ: 23°01.571'N; 57°59.906'E; 710 m

summit of MTZ: 23°01.361'N; 58°00.184'E; 730 m

-Khilah outcrop

base of MTZ: 22°59.755'N; 57°59.073'E; 750 m

summit of MTZ: 22°59.564'N; 57°59.327'E; 840 m

-11OA48

base of MTZ: 23°0.667'N; 57°59.73'E; 820 m

summit of MTZ: 23°0.467'N; 57°59.75'E; 870 m

-95OD116

base of MTZ: 23°0.48'N; 57°57.572'E; 930 m

summit of MTZ: 23°0125'N; 57°57.538'E; 1180 m

-11OA57

base of MTZ: 23°02.862'N; 57°55.293'E; 910 m

summit of MTZ: 23°03.003'N; 57°55.285'E; 1020 m

-11OA28

base of MTZ: 23°05.074'N; 57°55.415'; 1018 m

summit of MTZ: 23°05.065'N; 57°55.371'E; 1045 m

-11OA20

base of MTZ: 23°05.235'N; 57°55.501'E; 1000 m

summit of MTZ: 23°05.241'N; 57°55.462'E; 1020 m

-11OA18

base of MTZ: 23°05.65'N; 57°55.509'E; 1090 m

summit of MTZ: 23°05.646'N; 57°55.47'E; 1120 m

-11OA10

base of MTZ: 23°05.548'N; 57°55.535'E; 1060 m

summit of MTZ: 23°05.55'N; 57°55.475'E; 1115 m

-11OA1

base of MTZ: 23°05.98'N; 57°55.23'E; 960 m

summit of MTZ: 23°05.97'N; 57°55.1'E; 1060 m

-12OA21

base of MTZ: 23°06.999'N; 57°54.408'E; 950 m

summit of MTZ: 23°07.046'N; 57°54.249'E; 1000 m

Fig. 4a: 23°04.47'N; 57°59.92'E; Fig. 4b: 23°01.4'N; 57°59.84'E;

Fig. 4c: 23°00.75'N; 57°59.76'E; Fig. 4d: 22°59.62'N; 57°59.62'E;

Fig. 4e: 23°06.25'N; 57°56.62'E; Fig. 4f: 23°01.5'N; 58°00'E

Fig. 4 g/h: 23°02.5'N; 58°00.1'E.

Methods

Our field investigations show that the base of the MTZ often does not match that picked on photographs from Google Earth, even when guided by the BRGM-Oman ministry of industry map, so the altitude of the base of the MTZ was constrained by field observations only. On the other hand, we verified in the field that we were able to correctly pick the Moho on aerial photographs; this allowed us to complement field observations of the base of the MTZ, with the Moho altitude picked on photographs, and constrain the MTZ thickness at 24 locations, in addition to our 15 logs (figure DR1). Despite the imprecision mentioned above, we attempted to continuously define the

base and summit of the MTZ on Google-Earth photographs. This map was imported into the Gocad modeling software (available from the Paradigm Geophysical company) and superimposed on a digital elevation model (DEM) of the area obtained from the Advanced Spaceborne Thermal Emission and Reflection Radiometer Global Digital Elevation Map program. The DEM accuracy is estimated to be 20 meters at 95% confidence for vertical data, and 30 meters at 95% confidence for horizontal data, and the dip of our picked surfaces on Google-Earth views seems coherent with the dip in the numerical model. From our picking, we derived three-dimensional surfaces of the base and top of the MTZ (figure DR2). To do so, the Gocad software uses the discrete smooth interpolation method, which is tailored for geological objects (Caumon et al, 2009). Logs in the northern part show that the Moho is close to 1000 meters altitude; however hills along the spreading axis reach that altitude with harzburgite cropping out at their summit, demonstrating doming of the Moho along the axis. In our first MTZ model, the Moho was predicted to cross the on-axis hills; thus an uphill slope towards the axis was needed for the limits of the MTZ to take into account the doming effect. Although the BRGM-Oman Ministry of Industry map shows some fractured contacts between the base of the MTZ and the harzburgite, no fault is required to accommodate the geometry of the MTZ.

Reference in supplemental information

Caumon, G., Collon-Dreuillet, P., De Veslud, C. L. C., Viseur, S. & Sausse, J.. Surface-based 3D modeling of geological structures. *Mathematical Geosciences*, 41(8), 927-945 (2009).

Figure caption in supplemental information

Figure DR1: a) 15 logs of the upper mantle section and MTZ in the Maqsad region b) location of the logs within a simplified lineation map of the Maqsad diapir.

Figure DR2: a) illustration of the picking of the MTZ boundaries on an aerial photograph; b) same view as in 2a in our DEM (pink is the topography, green surface is the base of the MTZ, yellow surface is the top of the MTZ/base of the crust. The location of this view is shown on figure DR1.

c-d) global views of the interpolated base and top surface of the MTZ throughout the area.

Figure DR3: photograph of the thin section sketched in Fig. 4a

Journal Pre-proof

Credit author statement

David Jouselin initiated the project, participated to the field work (2 field campaigns), participated to the aerial photo survey, supervised the modeling, wrote the article

Adolphe Nicolas initiated the project, participated to the field work (2 field campaigns), commented on the article

Françoise Boudier initiated the project, participated to the field work (2 field campaigns), commented on the article

Laurie Reisberg participated to the field work (1 field campaign), commented on the article

Mathilde Henri participated to the aerial photo survey, did the modeling and commented on the article

Marie Nicolle participated to the field work (1 field campaign), commented on the article

Journal Pre-proof

Declaration of interests

The authors declare that they have no known competing financial interests or personal relationships that could have appeared to influence the work reported in this paper.

Journal Pre-proof

Highlights

In Oman ophiolite, Moho transition zone (MTZ) below the crust made of reactive dunite

MTZ grows to peak thickness (500 meters) 6 km away from ridge axis

Melt-free dunite acts as barrier for ascending melt, which accumulates at base of MTZ

Accumulated melt turns uppermost harzburgite into dunite, thickening the dunite layer

We predict sub-Moho melt lenses at growing depth with distance from oceanic ridges

Journal Pre-proof

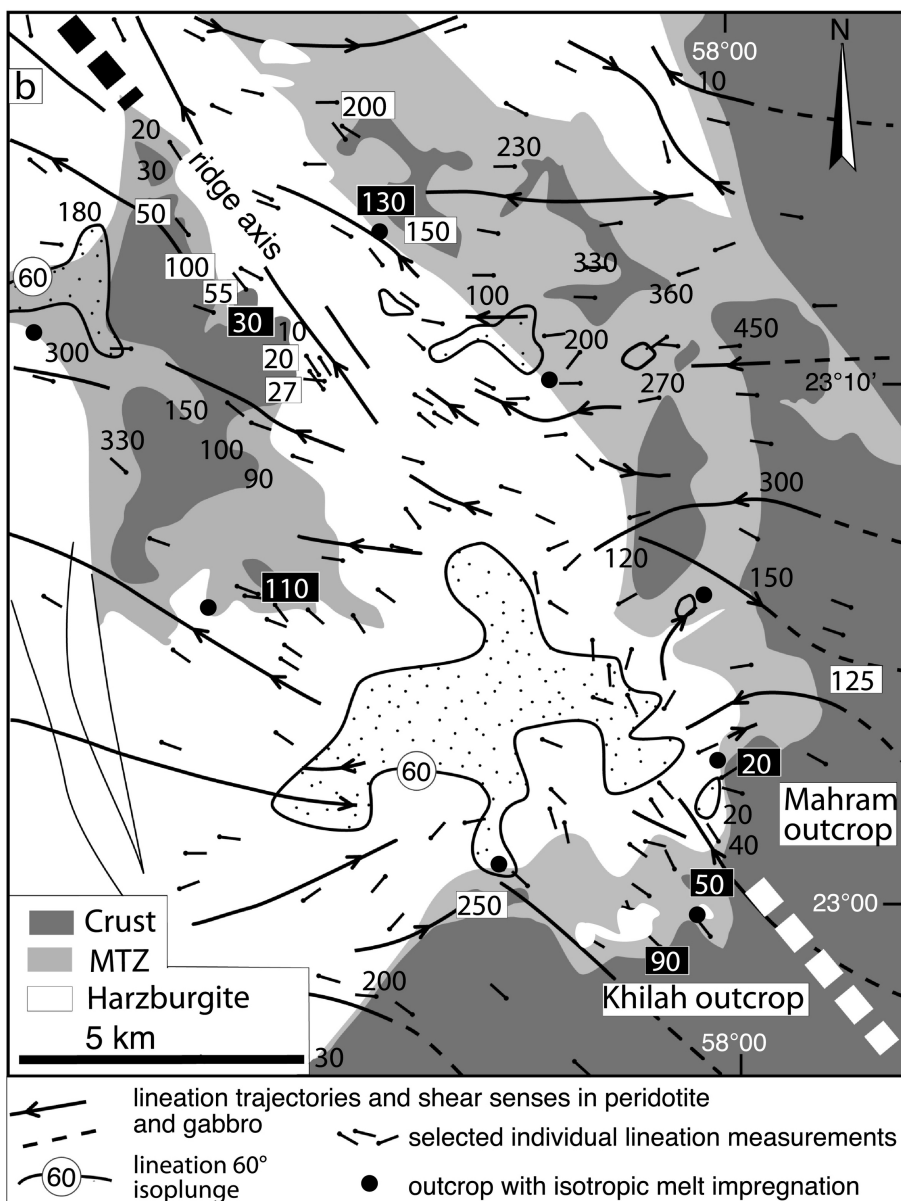
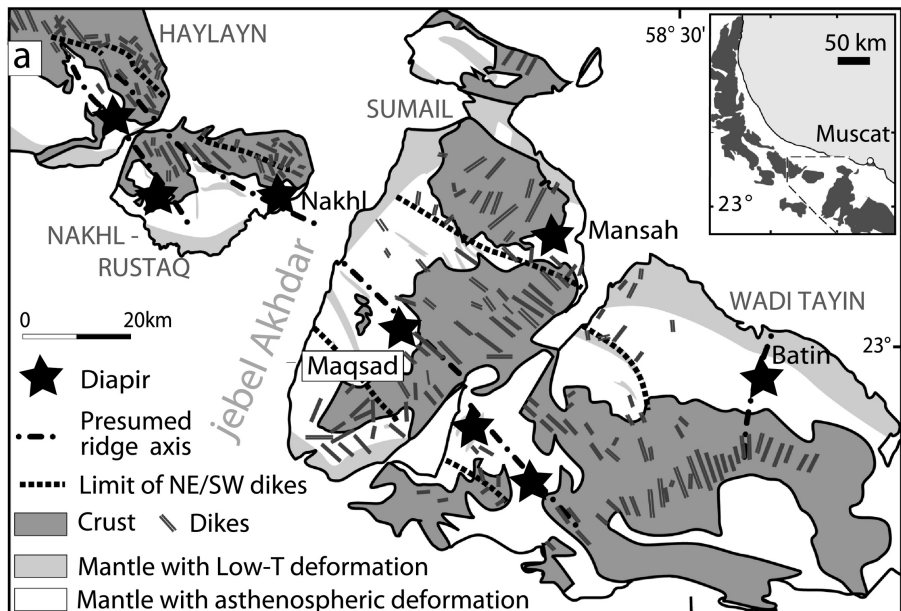


Figure 1

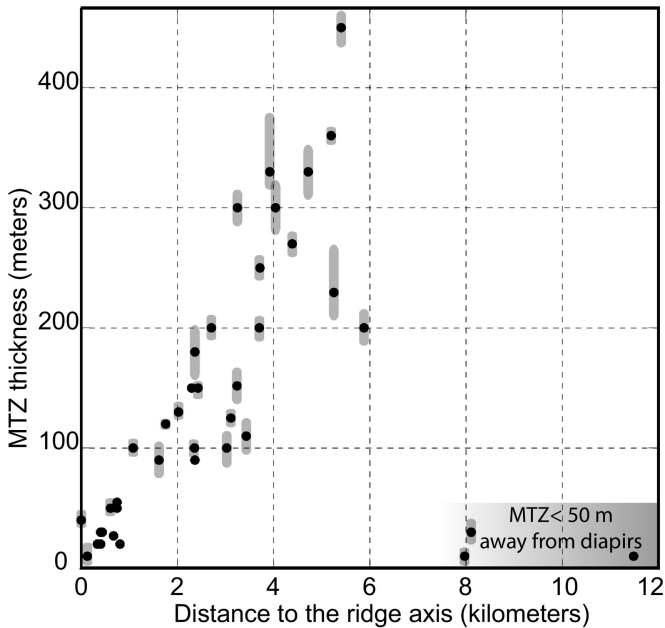


Figure 2

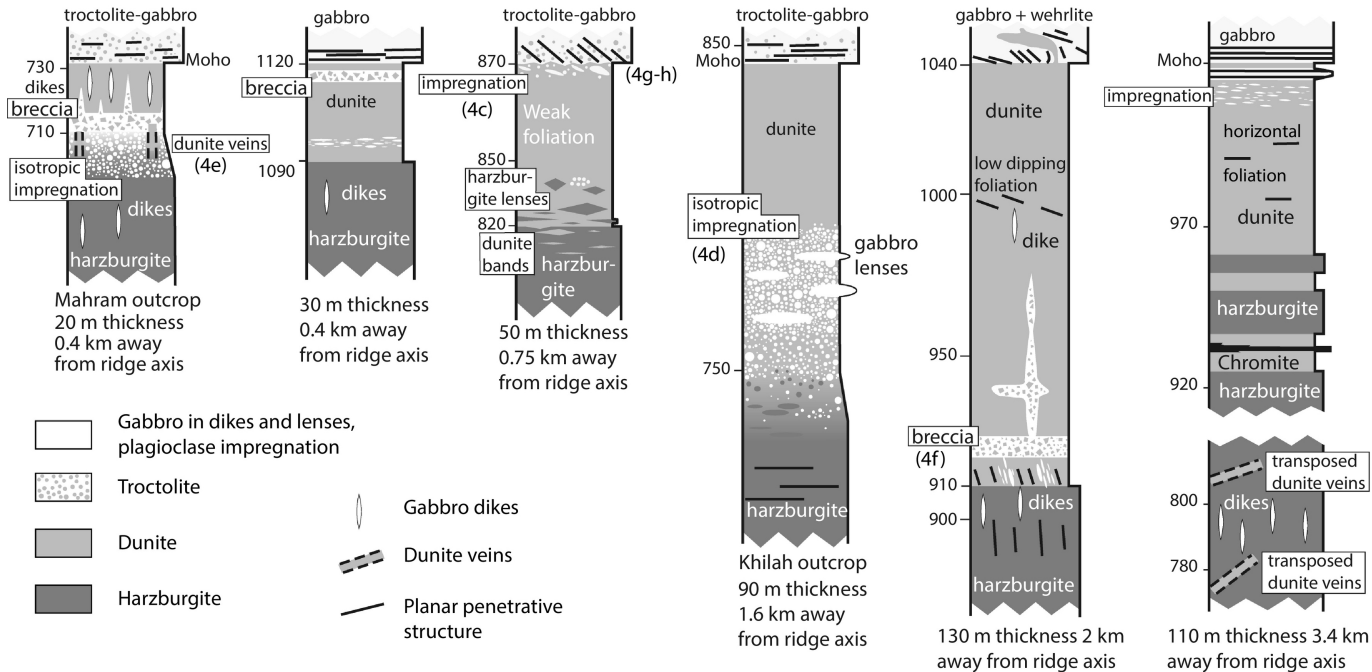


Figure 3

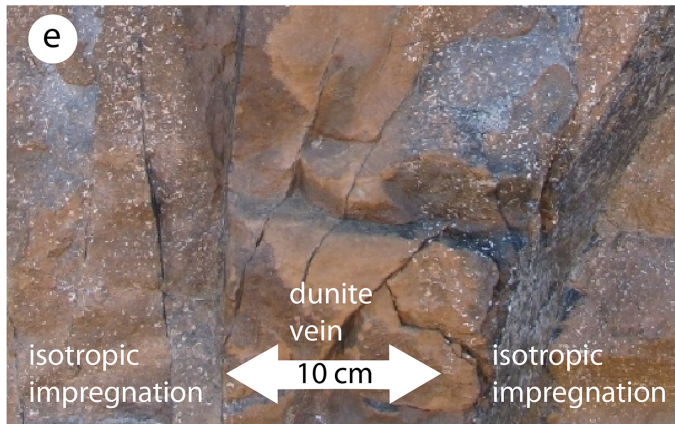
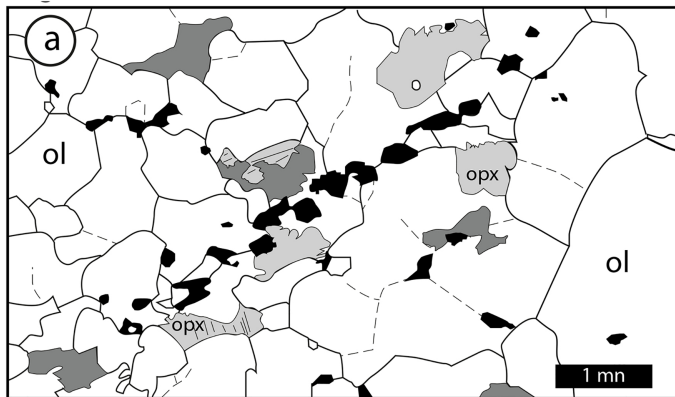


Figure 4

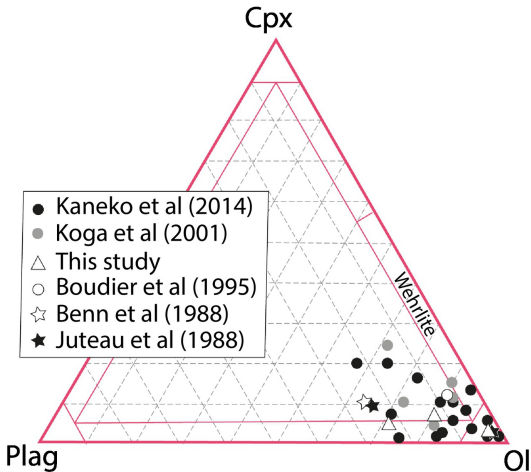


Figure 5

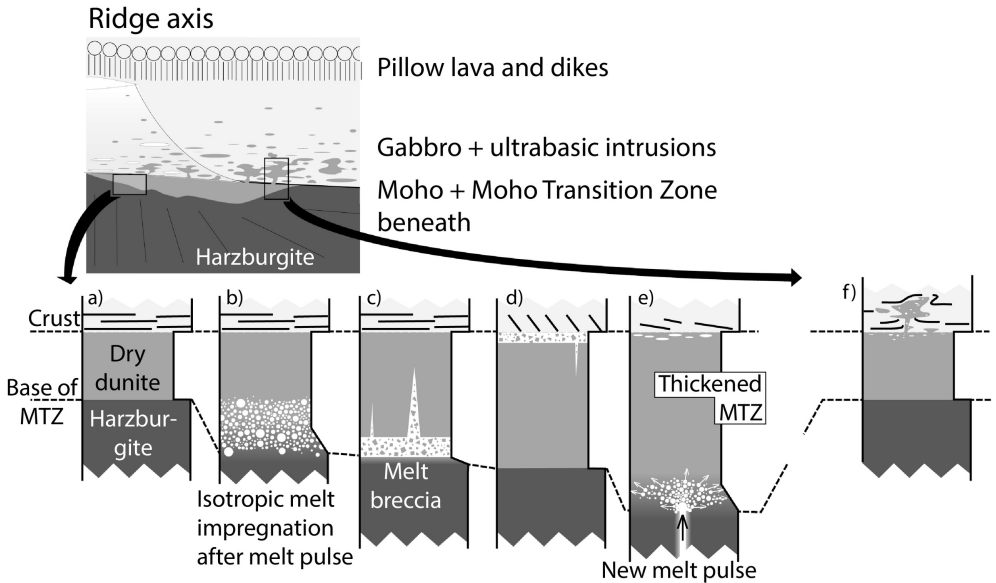


Figure 6

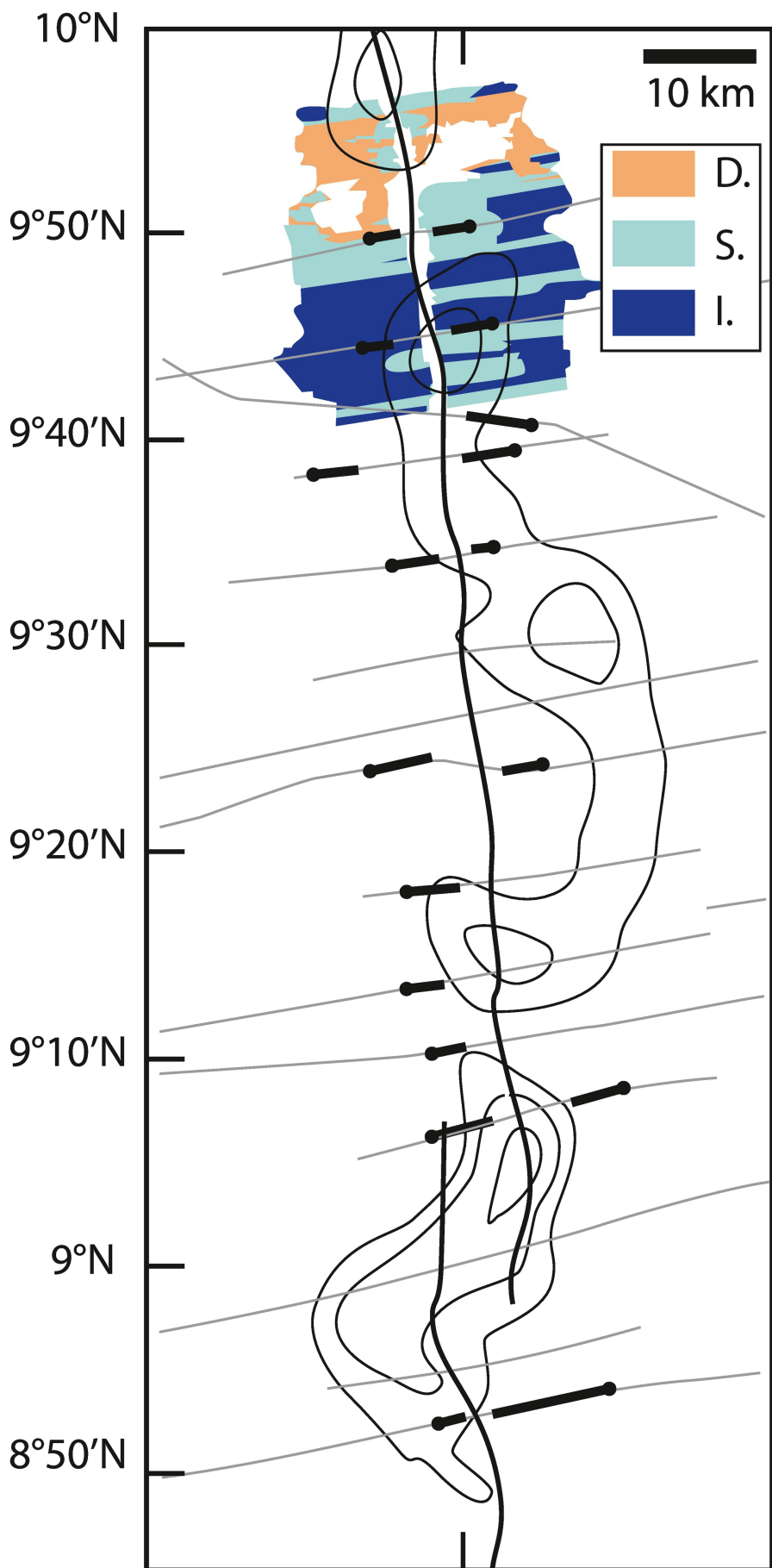


Figure 7